



ELSEVIER

Contents lists available at ScienceDirect

## Materials Letters

journal homepage: [www.elsevier.com/locate/matlet](http://www.elsevier.com/locate/matlet)

# Morphologies and plane indices of pyramid patterns on wet-etched patterned sapphire substrate



Yu-Chung Chen<sup>a</sup>, Bo-Wen Lin<sup>a,b</sup>, Wen-Ching Hsu<sup>c</sup>, YewChung Sermon Wu<sup>a,\*</sup>

<sup>a</sup> Department of Materials Science and Engineering, National Chiao Tung University, Taiwan

<sup>b</sup> Crystalwise Technology Inc., Hsinchu 30077, Taiwan

<sup>c</sup> Sino-American Silicon Products Inc., Hsinchu 30075, Taiwan

## ARTICLE INFO

## Article history:

Received 24 September 2013

Accepted 7 December 2013

Available online 17 December 2013

## Keywords:

Patterned sapphire substrate

Wet etching process

Crystal structure

Optical materials

Properties

Surfaces

## ABSTRACT

A wet etching process was employed to investigate the evolution of pyramids on the patterned sapphire substrate (PSS). It has been found that the PSS comprised a hexagonal pyramid covered with six facets  $\{3\bar{4}17\}$  when disk-shaped  $\text{SiO}_2$  mask still remained. Three facets  $\{1\bar{1}05\}$  were exposed when mask was etched away. In this study, a continuous etching process was performed. It was found that another six facets  $\{4\bar{5}130\}$  and another three facets  $\{1\bar{1}010\}$  appeared on the bottom and the top of pyramid. Finally, when the etching time reached around 5 min, most of pyramids on the PSS disappeared.

© 2013 Elsevier B.V. All rights reserved.

## 1. Introduction

Light-emitting diodes (LEDs) are expected to play an important role in the next-generation light source. Many techniques have been developed for improving internal quantum efficiency (IQE) and light extraction efficiency (LEE). Patterned sapphire substrate (PSS) is one of these efforts. This is because most of the growth of GaN was initiated from *c*-planes. As the growth time increased, GaN epilayers on the bottom *c*-plane covered patterns by lateral growth causing the threading dislocation to bend toward the patterns resulting in the improvement of epilayer quality and IQE [1–3]. Besides, these patterns can redirect photons, which were originally emitted out of the escape cone, back into the escape cone. As a result, LEE was improved [3–5].

In wet etching PSS, the sapphire substrate covered with the  $\text{SiO}_2$  hard mask is usually etched by a mixed solution of hot  $\text{H}_2\text{SO}_4$  and  $\text{H}_3\text{PO}_4$ . After etching, several etched facets were exposed. It was found that when the  $\text{SiO}_2$  mask still remained on the top *c*-plane, the PSS structure comprised a hexagonal pyramid covered with six facets (6B)  $\{3\bar{4}17\}$  with a flat top *c*-plane [6]. However, when the  $\text{SiO}_2$  mask was etched away, there were three more facets (3T)  $\{1\bar{1}05\}$  exposed on the top.

This study investigated the evolution of these pyramids on PSS using a continuous *two-step* etching process.

## 2. Experimental

The two-step wet etching process is illustrated in Fig. 1. For the first-step etching, sapphire substrate with  $\text{SiO}_2$  hard mask was immersed in a mixture etchant of  $\text{H}_2\text{SO}_4:\text{H}_3\text{PO}_4$  (3:1) at  $270^\circ$  for 8 min. It was designated as “8PSS”. The 8PSS was then dipped into buffered oxide etchant (BOE) to remove the  $\text{SiO}_2$  mask. Samples were then etched in the same solution for various durations. It was designated as “*t*+8PSS”, where *t* denotes the second-step etching time. The surface morphology was analyzed using scanning electron microscope (SEM), and that cross-sectional SEM inspection was achieved after localized etching by focused ion beam.

## 3. Results and discussion

After the first-step etching for 8 min, the structure of 8PSS comprised a hexagonal pyramid covered with six facets (6B)  $\{3\bar{4}17\}$  with a flat top *c*-plane. Then,  $\text{SiO}_2$  mask was removed for the second-step etching. Fig. 2 shows the SEM images of 8PSS after the second-step etching for 1 to 5 min. Three 3T facets  $\{1\bar{1}05\}$  were found on the top of 6B facets, as shown in Fig. 2(a) and (b) [6].

When etching time reached 2 min (2+8PSS), six “low-6-bottom” (L6B) planes appeared on the bottom of pyramids (Fig. 2(c) and (d)). When the second-step etching time was 3 min (3+8PSS), 3T facets vanished and three other facets were found on the top of L6B

\* Corresponding author.

facets, as shown in Fig. 2(e). These three facets were designated as “low-3-top” (L3T) planes. The L6B disappeared after 4-min etching, as shown in Fig. 2(g). After 5-min etching, most of pyramids on the PSS vanished as shown in Fig. 2(h).

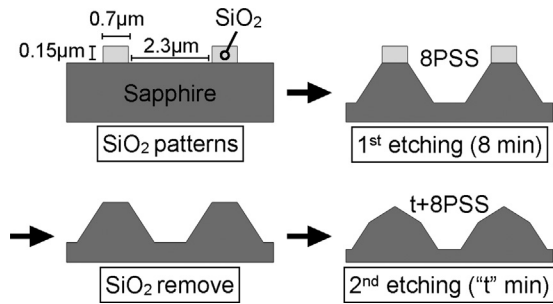


Fig. 1. The flow chart of two-step wet etching process.

Part of the evolution of 6B and 3T has been investigated in our previous study [6]. When SiO<sub>2</sub> mask remained, the etching rate of 6B planes was very slow. However, when mask was removed, 3T facets appeared. As a result, with increase in etching time, the size (height) of pyramids decreased while the 3T areas increased.

The detail of pyramid evolution during the second-step etching was schematically illustrated in Fig. 3. After about 1.5 min, 3T facets would touch the bottom c-plane (Fig. 3(a)). Then, L6B facets appeared on the intersection of 6B, 3T and bottom c-plane (Fig. 3(b)). With increase in etching time, the areas of L6B facets increased while those of 3T and 6B decreased. At the same time, the size of pyramids decreased (Fig. 3(a)–(c)). As the etching time increased, reached around 2.7 min, the 3T areas vanished (Fig. 3(d)). The pyramids were covered by six L6B facets. Then, L3T facets appeared on the top of pyramids (Fig. 3(e)). With the increase of etching time, the area of L3T increased, while that of L6B decreased (Fig. 3(d)–(f)). The size of pyramid continued to decrease. Finally, the L3T facets were dominant and disappeared gradually. The study of etching rates followed the

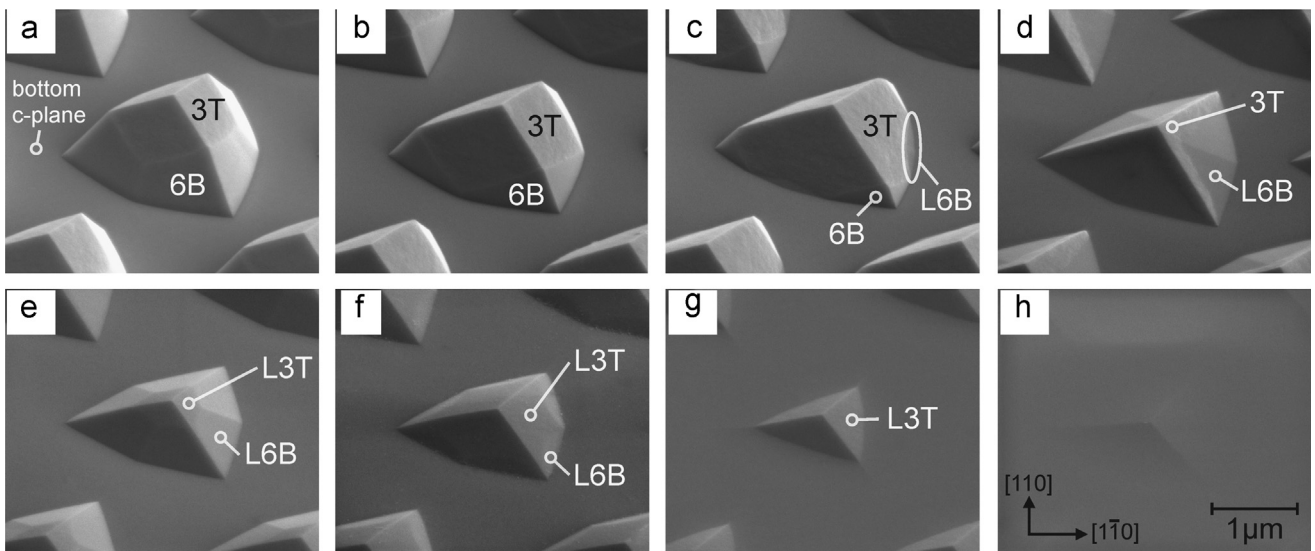


Fig. 2. SEM side-view images of (a) 1+8PSS, (b) 1.5+8PSS, (c) 2+8PSS, (d) 2.5+8PSS, (e) 3+8PSS, (f) 3.5+8PSS, (g) 4+8PSS and (h) 5+8PSS (viewed from 52° to sample normal).

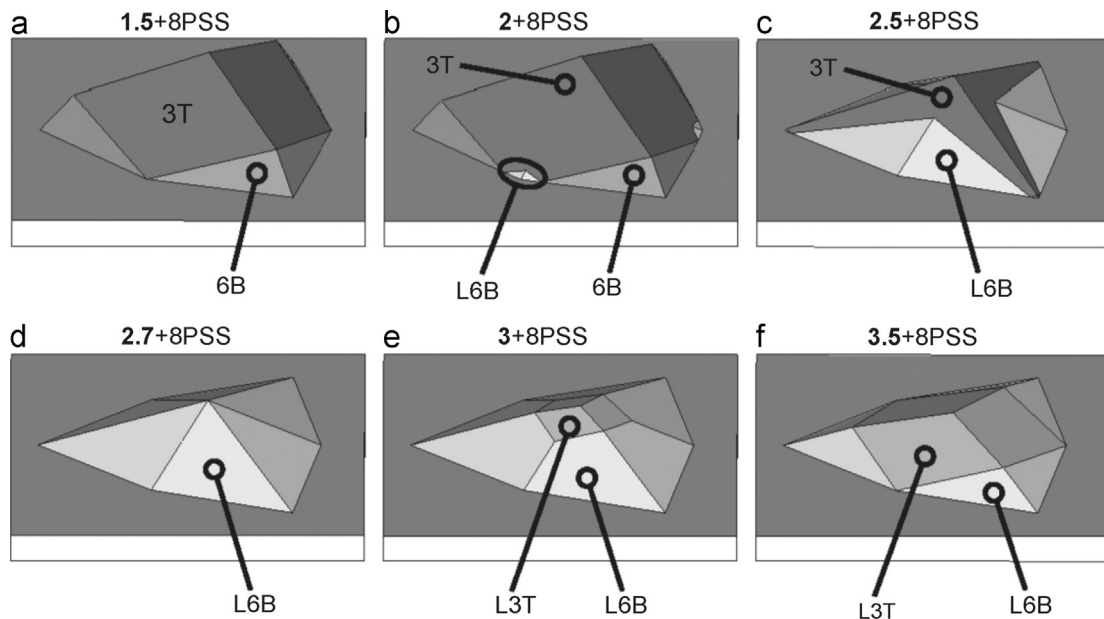


Fig. 3. The detail of pyramid evolution during the second-step etching.

approach described in Ref. [6]. The etching rates of 6B, 3T, L6B and L3T were about 0, 0.22, 0.09 and 0.20  $\mu\text{m}/\text{min}$ , respectively.

The study of plane indices of L6B and L3T followed the approach described in Refs. [6,7]. Before built 3-dimension (3D) models for L6B and L3T facets, several related angles were measured. The projection of 2.5+8PSS pyramid on the (0001) plane is shown in Fig. 4(a). Two intersection directions of L6B planes and c-plane were indicated by two white lines. The measured angle between these two lines was  $82^\circ$ . The slanted angle between L6B facet and c-plane was measured around  $25^\circ$  as shown in Fig. 4(b). On the other hand, the projection of L3T pyramid is shown in Fig. 4(c). The measured angle was  $60^\circ$ , while the slanted angle between L3T facet and c-plane was  $17^\circ$  as shown in Fig. 4(d).

Based on these angles, 3D models of L6B and L3T pyramids are schematically illustrated in Fig. 5. The intercepts of L6B and L3T planes on  $a_1$ -,  $a_3$ - and c-axis were measured. Then, the reciprocals of these numbers were multiplied with the sapphire's unit length

( $a=4.759 \text{ \AA}$  and  $c=12.991 \text{ \AA}$ ). As a result, the calculated Miller-Bravais indices of L6B and L3T planes were  $\{4\bar{5}130\}$  and  $\{1\bar{1}010\}$ , respectively.

These L6B and L3T plane indices were confirmed by calculating the angles among L6B, L3T and c-planes [6,7]. Before confirming the angle between L6B planes and c-plane, the intersection directions of L6B planes were calculated. One of these directions was  $[\bar{1}0103]$  as shown in Fig. 5(a). The calculated angle between  $[\bar{1}0103]$  and  $[001]$  (normal direction of c-plane) was  $64.7^\circ$ . In other words, the cross-sectional slanted angle was  $25.3^\circ$ , which was almost the same as those angles observed in Fig. 4(b). Two intersection directions of L6B planes and c-plane were calculated by the cross product of normal directions of these planes [7] They were  $[1\bar{4}0]$  and  $[\bar{5}40]$ . The calculated angle between these two directions was  $81.8^\circ$ , which was almost the same as those angles observed in Fig. 4(a). On the other hand, the calculated angle between L3T planes and c-plane (0001) was  $17.5^\circ$ , and between the intersection directions of L3T planes and c-plane was  $60^\circ$ ,

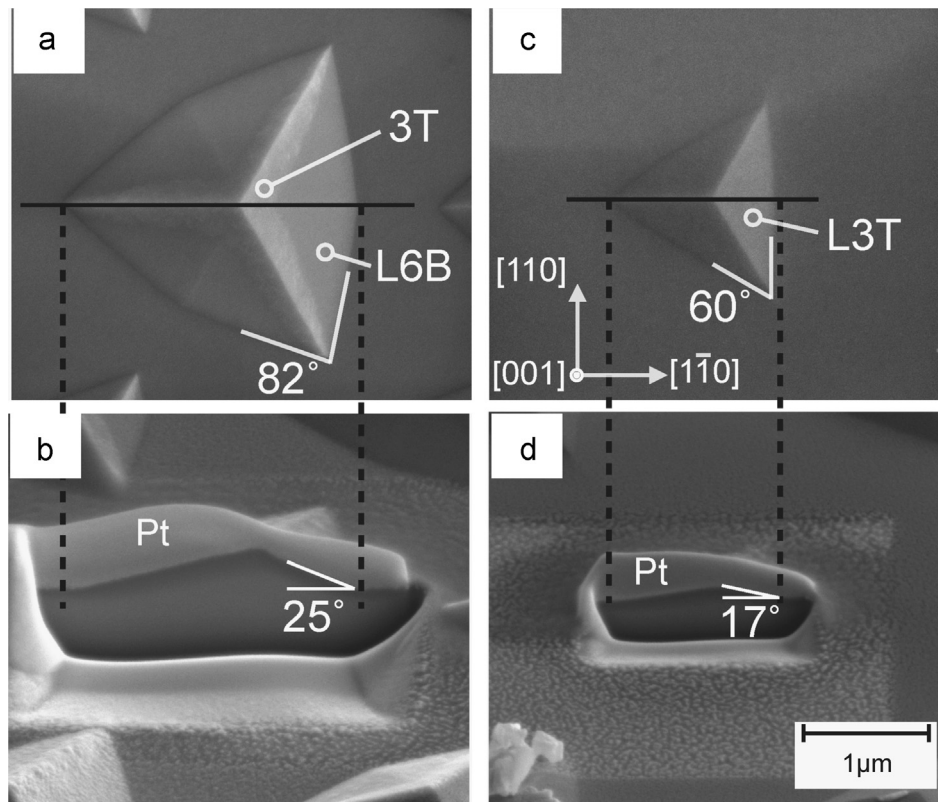


Fig. 4. SEM images of 2.5+8PSS. (a) Top-view image. (b) Side-view of the cross-sectional illustration from (a) indicated by black lines. SEM images of 4+8PSS. (c) Top-view image. (d) Side-view of the cross-sectional image.

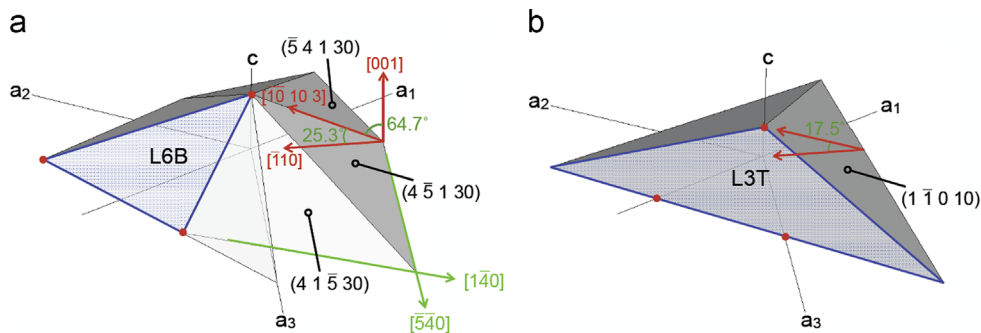


Fig. 5. Schematic illustrations of (a) 2.7+8PSS and (b) 4+8PSS.

which were almost the same as those angles observed in Fig. 5 (d) and (c), respectively.

#### 4. Conclusions

Wet etching of PSS has been employed to improve both IQE and LEE of GaN-based LEDs. Several etched facets were exposed on the PSS. In this study, a two-step wet etching process was employed to investigate the evolution of these facets on the PSS. The substrate with the SiO<sub>2</sub> mask was immersed in a H<sub>3</sub>PO<sub>4</sub>-based etchant at 270° for various durations. When the SiO<sub>2</sub> mask remained on the top *c*-plane, PSS has hexagonal pyramid structures covered with six 6B facets {3  $\bar{4}$  1 7}. When the SiO<sub>2</sub> mask was etched away, three 3T facets {1  $\bar{1}$  0 5} were found on the top. With increase in etching time, other six L6B facets {4  $\bar{5}$  1 30} appeared on the bottom of pyramids. When the second-step etching time reached 3 min, another three L3T facets {1  $\bar{1}$  0 10} were found on the top. Finally, when the etching time reached around 5 min, most of pyramids on the PSS disappeared.

#### Acknowledgments

This project was funded by Sino American Silicon Products Incorporation and the National Science Council of the Republic of

China under Grant no. 101-2221-E-009-052-MY3. Technical support from the National Nano Device Laboratory, Center for Nano Science and Technology, Nano Facility Center and Semiconductor Laser Technology Laboratory of the National Chiao Tung University is also gratefully acknowledged.

#### References

- [1] Yu NS, Guo LW, Chen H, Xing ZG, Ge BH, Wang J, et al. Near ultraviolet InGaN/GaN MQWs grown on maskless periodically grooved sapphire substrates fabricated by wet chemical etching. *J Alloys Compd* 2007;428:312–5.
- [2] Oh TS, Jeong H, Lee YS, Seo TH, Park AH, Kim H, et al. Defect structure originating from threading dislocations within the GaN film grown on a convex patterned sapphire substrate. *Thin Solid Films* 2011;519:2398–401.
- [3] Wu DS, Wang WK, Wen KS, Huang SC, Lin SH, Horng RH, et al. Fabrication of pyramidal patterned sapphire substrates for high-efficiency InGaN-based light emitting diodes. *J Electrochem Soc* 2006;153:G765–70.
- [4] Xu C, Yu T, Yan J, Yang Z, Li X, Tao Y, et al. Analyses of light extraction efficiency in GaN-based LEDs grown on patterned sapphire substrates. *Phys Status Solidi (c)* 2011;9:757–60.
- [5] Lee YJ, Lu TC, Kuo HC. High brightness GaN-based light-emitting diodes. *J Disp Technol* 2007;3:118–25.
- [6] Chen YC, Hsiao FC, Lin BW, Wang BM, Wu YS, Hsu WC. The formation and the plane indices of etched facets of wet etching patterned sapphire substrate. *J Electrochem Soc* 2012;159:D362–6.
- [7] Lee WE, Lagerlof KPD. Structural and electron diffraction data for sapphire ( $\alpha$ -Al<sub>2</sub>O<sub>3</sub>). *J Electron Microscop Tech* 1985;2:247–58.